



# Strong diurnal variability of carbon dioxide flux over algae-shellfish aquaculture ponds revealed by eddy covariance measurements

Yiping Zhang<sup>a,b,c</sup>, Xianghui Guo<sup>a,d</sup>, Xudong Zhu<sup>a,b,c,d,e,\*</sup>

<sup>a</sup> State Key Laboratory of Marine Environmental Science, Xiamen University, Xiamen, Fujian Province, China

<sup>b</sup> Key Laboratory of the Coastal and Wetland Ecosystems (Ministry of Education), Xiamen University, Xiamen, Fujian Province, China

<sup>c</sup> College of the Environment and Ecology, Xiamen University, Xiamen, Fujian Province, China

<sup>d</sup> National Observation and Research Station for the Taiwan Strait Marine Ecosystem (Xiamen University), Zhangzhou, Fujian Province, China

<sup>e</sup> Southern Marine Science and Engineering Guangdong Laboratory (Zhuhai), Zhuhai, Guangdong Province, China

## ARTICLE INFO

### Keywords:

Carbon dioxide  
Diurnal variation  
Aquaculture  
Razor clam  
Zhangjiang  
Eddy covariance

## ABSTRACT

Aquaculture ponds represent a biogeochemical hotspot of the global carbon cycle. However, accurate estimations of their carbon budgets are hindered by a limited understanding of the temporal variability of carbon fluxes across time scales. In this study, the eddy covariance (EC) approach was applied to quantify net ecosystem CO<sub>2</sub> exchange (NEE) over algae-shellfish aquaculture ponds (razor clam cultivation) in Zhangjiang Estuary of Southeast China from January 2020 to June 2022, aiming to assess the diurnal variability of NEE during various management periods. The EC-based NEE over the ponds showed strong diurnal variations with daytime sink and nighttime source, mainly controlled by photosynthetically active radiation and air temperature, respectively. The ponds acted as a net sink system during razor clam (daily mean flux of  $-0.42 \mu\text{mol m}^{-2} \text{s}^{-1}$ ) and shrimp-crab ( $-0.50 \mu\text{mol m}^{-2} \text{s}^{-1}$ ) farming periods with a stronger daytime sink than a nighttime source, while it was the opposite during the drainage period acting as a net source ( $0.40 \mu\text{mol m}^{-2} \text{s}^{-1}$ ). The strength of sink/source also differed between the early and late stages of the razor clam farming period, with much larger ( $\sim 16$  times) net carbon uptake in the late stage as a result of the strong daytime sink and near-neutral nighttime flux. The diurnal variability of NEE over the ponds was overall larger than other aquatic ecosystems and tended to increase with air temperature. Previous estimates of daily NEE from discrete daytime-only samplings might have biased the actual carbon budgets if no diurnal correction was applied in the temporal aggregation. The confirmed strong temporal variability of NEE across time scales highlighted the importance and necessity of continuous and high-frequency flux measurements in assessing the carbon budgets of algae-shellfish aquaculture ponds.

## 1. Introduction

Carbon dioxide (CO<sub>2</sub>) is the most important anthropogenic greenhouse gas (GHG) accounting for approximately 60% of the atmospheric radiative forcing (IPCC, *in press*). Quantifying the strength of CO<sub>2</sub> sink/source for various ecosystems provides an essential foundation for mitigating CO<sub>2</sub> emissions (Friedlingstein et al., 2020). Despite numerous studies have concentrated on CO<sub>2</sub> fluxes across the water-air interface over various aquatic ecosystems, including lakes, rivers, and reservoirs (Baldocchi et al., 2020a; Gomez-Gener et al., 2021; Morin et al., 2022; Ran et al., 2022; Xiao et al., 2021), the CO<sub>2</sub> flux measurements over aquaculture ponds, particularly in a continuous and high-frequency manner, are very limited (Yang et al., 2019; Zhang et al., 2022a).

Aquatic ecosystems are often known as an important CO<sub>2</sub> source, and earlier estimates of the source from inland freshwaters were in the order of  $1.4 \text{ Pg C year}^{-1}$  (Tranvik et al., 2009), exceeding half of the terrestrial carbon sink. It has been increasingly recognized that the CO<sub>2</sub> emissions from aquatic ecosystems may have been underestimated due to the lack of incorporation of the contribution from small and shallow water bodies (Yuan et al., 2019; Zhang et al., 2022b). As one of such water bodies, aquaculture ponds are a vital part of the global aquatic ecosystems. Although aquaculture ponds occupy a very small area worldwide, they are found to play a crucial role in global carbon cycling (Yang et al., 2018b; Yuan et al., 2019). The estimated area of aquaculture ponds is  $\sim 1.8 \times 10^5 \text{ km}^2$  worldwide with China occupying the largest area ( $\sim 2.57 \times 10^4 \text{ km}^2$ ), and it is reported the area of aquaculture ponds in the

\* Corresponding author at: College of the Environment and Ecology, Xiamen University, Xiamen, Fujian Province, China.

E-mail address: [xdzhu@xmu.edu.cn](mailto:xdzhu@xmu.edu.cn) (X. Zhu).

Chinese coastal zone is  $1.56 \times 10^4 \text{ km}^2$  (FAO, 2019; Ren et al., 2019).

The characterization of GHG fluxes over aquaculture ponds in coastal areas has been carried out in numerous studies (David et al., 2021; Fang et al., 2022a; Xu et al., 2022; Yang et al., 2022; Zhang et al., 2022a). Compared with other aquatic ecosystems, aquaculture ponds, as semi-artificial ecosystems, usually have more complicated biogeochemical cycles affected by the combination of environmental drivers and aquaculture management. Aquaculture GHG fluxes can be strongly influenced by physical forcing, such as radiation (Zhang et al., 2022c) and temperature (Hu et al., 2020) at very short time scales (minutes to hours). Artificial management activities, such as feeding, water exchange, and harvesting, have also significantly added or removed carbon into or out of aquaculture ponds, which complicates the assessment of GHG fluxes (Fang et al., 2022b; Yang et al., 2018a). Different aquaculture farming systems may also introduce large discrepancies in GHG fluxes. For example, the fish ponds are often found to be a CO<sub>2</sub> source (Chen et al., 2016), while shrimp (Tong et al., 2021) and shellfish (Zhang et al., 2022c) aquaculture ponds in the coastal areas can act as a CO<sub>2</sub> sink.

Despite the high temporal variability of diurnal CO<sub>2</sub> flux regulated by multiple factors, most previous estimates of CO<sub>2</sub> flux relied on daytime-only sampling measurements that were carried forward into the temporal aggregation of seasonal or annual mean fluxes. Although a few studies have been conducted to examine the diurnal variations in CO<sub>2</sub> fluxes over aquaculture ponds (Chen et al., 2016; Hu et al., 2020), they are limited by imperfect flux measuring techniques that only permit measurements at several discrete time points or over short periods. At present, most CO<sub>2</sub> flux measurements over aquaculture ponds have been conducted manually using the floating chamber or boundary layer method (Chen et al., 2016; Yang et al., 2021). Although these approaches are good for understanding the spatial variability of CO<sub>2</sub> flux under various conditions, they fail to capture the high temporal variability of CO<sub>2</sub> flux over aquaculture ponds. Thus, the temporal variations of diurnal CO<sub>2</sub> flux over aquaculture ponds and its underlying mechanisms remain poorly understood. Continuous and high-frequency measurements of CO<sub>2</sub> flux at the ecosystem scale under various farming systems are indispensable to improve the understanding of temporal variation and the spatial upscaling of CO<sub>2</sub> fluxes over aquaculture ponds.

As an automatic, continuous, and non-destructive flux measuring technique, the eddy covariance (EC) approach serves as a good option to capture the high temporal variability of GHG fluxes (Baldocchi, 2020b). The EC approach has been increasingly applied in flux studies on aquatic ecosystems (Pu et al., 2022; Zhang et al., 2019). For examples, large methane emissions have been found in freshwater aquaculture ponds (Zhao et al., 2021), enclosure lake aquaculture (Pu et al., 2022), and shallow eutrophic lake (Xiao et al., 2017) based on multi-year EC measurements, and the EC-based CO<sub>2</sub> fluxes showed a strong diurnal variation with positive values at nighttime and negative values at daytime (Zhao et al., 2019); the seasonal variability of CO<sub>2</sub> fluxes from a lake has been well characterized by the EC measurements showing a sink in summer and a source in autumn (Baldocchi et al., 2020a); the EC measurements of both CO<sub>2</sub> and CH<sub>4</sub> fluxes in a small lake also confirmed the importance of continuous measurements to cover the seasonality of the flux (Gorsky et al., 2021). As shown in these studies, continuous measurements obtained from this technique is highly needed to enhance our mechanistic understanding of how different biotic and abiotic factors affect the diurnal variations in ecosystem-scale CO<sub>2</sub> flux in aquatic ecosystems.

The filter-feeding shellfish are known as ecosystem engineers to play crucial ecological roles (Alonso et al., 2021; Dong et al., 2022). The CO<sub>2</sub> fluxes over algae-shellfish aquaculture ponds (cultivating algae to feed shellfish) are temporally dynamic as regulated by complicated biotic and abiotic processes (Ye et al., 2022; Zhang et al., 2022c). In addition to photosynthesis and respiration processes, there is increasing evidence that the calcification process of shellfish growth can improve the CO<sub>2</sub>

sink capacity and affect the carbon cycle of the ecosystem (Han et al., 2017; Liu et al., 2022; Ren, 2021). However, little or no work has been conducted with continuous CO<sub>2</sub> flux measurements over aquaculture ponds during various farming periods, and thus the impact of different flux processes on carbon cycling remains controversial. Zhang et al. (2022c) has applied the EC approach to examine the temporal variations in air-water CO<sub>2</sub> fluxes over algae-shellfish aquaculture ponds, however their one-year EC measurements were not long enough to accurately assess the diurnal flux variability across various farming/management periods.

To the best of our knowledge, there is no such study on assessing the diurnal variability of net ecosystem CO<sub>2</sub> exchange (NEE) over algae-shellfish aquaculture ponds with various farming/management periods, based on multi-year, continuous, and high-frequency measurements. To fill this knowledge gap, the EC approach was applied to characterize the temporal variability of NEE over algae-shellfish aquaculture ponds in Zhangjiang Estuary of Southeast China from January 2020 to June 2022. The specific objectives are (1) to characterize the source/sink strength and the diurnal variability of NEE during various farming/management periods; (2) to compare the difference in the diurnal pattern of NEE among various periods; and (3) to explore possible mechanisms and implications of the diurnal pattern of NEE.

## 2. Materials and method

### 2.1. Study area

The study area was located in the aquaculture ponds in Zhangjiang Estuary of Southeast China (Fig. 1). This subtropical estuary experiences a semidiurnal tidal cycle with a mean tidal range of 2.1 m (Zhu et al., 2019) and a monsoonal climate with a mean annual rainfall of 1165.5 mm mostly from April to September and a mean annual air temperature of 22.4 °C (averaged from 2017 to 2021). These aquaculture ponds are located to the south of Zhangjiang river and comprised of paired algae and shellfish (razor clam) ponds with shallow water up to ~ 1 m. Razor clam (*Sinonovacula constricta*) is one of the dominant aquaculture farming types in coastal areas of China (Fisheries Department of Agriculture Ministry of China, 2021). These ponds are mainly used for razor clam farming roughly from September to May of the next year, and the rest of the time they are used for shrimp (*Penaeus*) and crab (*Scylla*) farming. During razor clam farming season, the pond water is routinely exchanged twice a day following the semi-diurnal tidal regime. At high tides, fresh tidal water is delivered into both algae and razor clam ponds, with the former being used for algae cultivation. At low tides, the razor clam pond is first drained and then filled with algae-rich water from the paired algae pond. Once razor clams have been harvested, the pond sediments are drained, ploughed, flattened, and left alone for about a week. Afterward, shrimp and crabs are cultured using aquatic feed pellets without extensive algae cultivation and water exchanges. This seasonal rotation of razor clam and shrimp-crab has been widely adopted by local farmers to avoid sediment degradations (e.g., humus accumulation and sediment compaction) as a result of continuous cultivation of razor clam. The production of razor clam in this study area is the highest in winter accounting for more than two thirds of the annual production (Wu et al., 2012).

### 2.2. Flux measurements

The NEE across the water-air interface of aquaculture ponds was measured with an eddy covariance (EC) system (Fig. 1a), mainly comprised of a three-axis sonic anemometer (CSAT-3, Campbell Scientific, Inc., Logan, UT, USA) and an open-path CO<sub>2</sub> gas analyzer (Li-7500, Li-COR Inc., Lincoln, NE, USA). The EC flux tower (23.9314°N, 117.4084°E; ChinaFLUX and USCCC) was built over aquaculture ponds with the EC system deployed ~ 5 m above the surface water (Zhang et al., 2022c), and the analyses of footprint climatology following

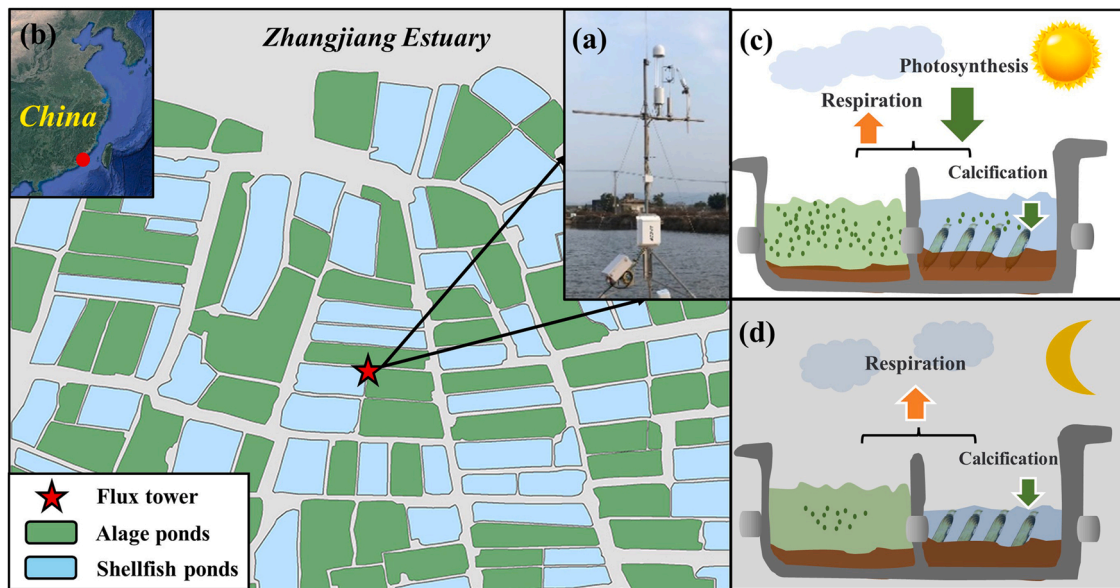


**Fig. 1.** The eddy covariance measurement system (a) deployed over algae-shellfish aquaculture ponds in Zhangjiang Estuary of Southeast China (b). Arrows with different sizes and directions indicate daytime (c) and nighttime (d)  $\text{CO}_2$  fluxes associated with photosynthesis, respiration, and calcification processes.

Kormann and Meixner (2001) confirmed that 90% of NEE was contributed by the ponds within  $\sim 400$  m around the tower (Fig. S1). Regular instrument maintenance including analyzer recalibration and drying chemicals renewals was conducted roughly every half year, and the sensor mirrors of the  $\text{CO}_2$  gas analyzer were manually cleaned once or twice a week to ensure credible signal strength. The raw EC measurements were recorded at a 10-Hz sampling rate and then processed into 30-min time series data through a standard procedure of EC flux corrections (including axis rotation, frequency response correction, ultrasonic correction, and WPL correction) and quality controls (including steady-state test, turbulent conditions test, statistical test, and absolute limits test) implemented in the EddyPro software (Li-COR Inc.) (Zhu et al., 2021a, 2021b). Each 30-min data was assigned a quality flag of 0, 1, or 2, standing for the best-, good- or poor-quality data, respectively (Mauder et al., 2013), and in this study, the data with a quality flag of 2 were excluded in further analyses. The 30-min data with rainfall or insufficient atmospheric mixing (friction velocity  $< 0.125 \text{ m s}^{-1}$ ) were also excluded. The percentage of valid 30-min NEE used in further data analyses over the study period (from January 2020 to June 2022) was 67.4%, in which daytime and nighttime data accounted for 37.2% and 30.2%, respectively. In this study, negative and positive values of NEE indicated a  $\text{CO}_2$  sink (downward air-to-water flux) and a  $\text{CO}_2$  source (upward water-to-air flux), respectively.

### 2.3. Ancillary measurements

Meteorological measurements over the study period included air temperature ( $T_a$ ), wind speed, photosynthetically active radiation (PAR), and rainfall.  $T_a$  and wind speed data were derived from the measurements of the three-axis sonic anemometer of the EC system. PAR and rainfall data were, respectively, measured with a PQSI PAR Quantum sensor (Kipp & Zonen, Delft, Netherlands) and a TE525MM rain gage (Campbell Scientific, Inc.) deployed on a nearby ( $\sim 1$  km away) mangrove flux tower. Water quality parameters measured in the algae pond under the EC system were also available from January to March 2021, including water temperature ( $T_w$ ), water level, pH, salinity, dissolved oxygen (DO), and Chlorophyll a (Chl-a).  $T_w$  and water level data were measured with a pressure sensor (HOBO U20L-04 Water Level Logger, Onset, Bourne, MA, USA). Water pH, DO, and Chl-a data were collected by a multi-parameter water quality analyzer (Aqua TROLL 500, In-Situ, Fort Collins, CO, USA). To ensure data quality, the water

quality analyzer was regularly cleaned and calibrated before each re-deployment every month during our site visit. To match the EC data, all ancillary measurements were consistently converted into 30-min time series for further analyses.

### 2.4. Statistical analyses

To reduce the bias in the temporal aggregation from 30-min to daily or monthly values due to unbalanced data gaps between daytime and nighttime, the aggregations were first conducted respectively for daytime and nighttime and then combined to produce daily or monthly fluxes. The daytime/nighttime timing was determined using a PAR threshold of  $10 \mu\text{mol m}^{-2} \text{ s}^{-1}$  (Zhu et al., 2021c). The temporal aggregation was calculated by multiplying the average by its aggregation duration. Any daytime or nighttime with valid 30-min values of less than one-fourth was excluded in the temporal aggregation (6.25% of daytime and 6.47% of nighttime were excluded). To quantitatively compare the difference between daytime and nighttime fluxes, we defined a diurnal variability factor of  $V_{DN}$  calculated as the absolute value of the ratio of the difference between daytime and nighttime NEE over daytime NEE:  $V_{DN} = |(NEE_{\text{daytime}} - NEE_{\text{nighttime}}) / NEE_{\text{daytime}}|$ . To estimate the influence of the daytime-only flux measurement on the temporal aggregation, we also derived a diurnal correction factor (Sieczko et al., 2020) of  $C_{DN}$  calculated as the ratio of mean daily (daytime and nighttime) NEE over mean daytime NEE:  $C_{DN} = NEE_{\text{day\_mean}} / NEE_{\text{daytime\_mean}}$ . Both  $V_{DN}$  and  $C_{DN}$  were calculated for four seasons and the drainage period, as well as various farming periods including early (from October to December) and late (from January to April) stages of the algae-shellfish period and the shrimp-crab period. The timing of various farming and drainage periods was determined mainly based on general farming practices applied in the study area and personal communication with local farmers. The correlations between NEE and environmental factors were examined using Pearson correlation analysis. All the data calculations and analyses were implemented using MATLAB software (MathWorks, Inc., Natick, MA, USA).

### 3. Results

#### 3.1. Temporal variations in environmental factors

The temporal variations in daily meteorological variables from January 2020 to June 2022 was shown in Fig. 2. The temporal variation in daily cumulative PAR showed a strong day-to-day fluctuation and a clear seasonality ranging from 13.8 to 65.8 mol m<sup>-2</sup> day<sup>-1</sup> (Fig. 2a). Daily mean wind speed had a weak seasonality with a mean value of 2.43 m s<sup>-1</sup> (varying from 0.62 to 5.56 m s<sup>-1</sup>). Daily mean Ta and Tw exhibited similar seasonal variations with the maximum and minimum values in August and January, respectively. During the study period, they had an average of 23.3 °C (from 5.6 to 32.8 °C) and 24.6 °C (from 5.8 to 34.3 °C), respectively. Approximately two-thirds of annual rainfall occurred within four months (May, June, August, and September) over the study period with maximum daily rainfall of 104.8 mm.

The mean diurnal variation in 30-min measurements showed distinct diurnal patterns in environmental factors, where on average PAR, wind speed, Ta, and Tw peaked at ~ noon, ~3 pm, ~1 pm, and ~3 pm respectively (Fig. 3). The diurnal variations of PAR were similar among seasons showing single-peak diurnal patterns, but the intensity of PAR differed among seasons with the highest (1508.7 μmol m<sup>-2</sup> s<sup>-1</sup>) and lowest (1092.7 μmol m<sup>-2</sup> s<sup>-1</sup>) midday PAR in summer and winter, respectively. Diurnal wind speed varied from 1.56 to 3.89 m s<sup>-1</sup>, with obviously stronger afternoon winds for all seasons. Afternoon winds were stronger in spring and winter, while nighttime winds were stronger in autumn and winter. Diurnal patterns of both Ta and Tw were similar among seasons, but on average the summer-winter temperature difference was 12.9 °C and 13.6 °C for Ta and Tw, respectively. Also, the timing of peaking values between Ta and Tw was different, where the peak values of Tw were ~ 2 h lagging behind those of Ta.

The 30-min water parameters measured in the algae pond showed significant diurnal variations from January to March 2021 (Fig. 4). The pH and DO shared a similar diurnal pattern with higher values in the

afternoon (Fig. 4b-c), where pH ranged from 6.45 to 9.45 (average of 8.52) and DO ranged from 0 to 21.5 mg L<sup>-1</sup> (average of 8.79 mg L<sup>-1</sup>). The water level and Chl-a were averaged at 0.38 m (from 0 to 0.65 m) and 200.0 μg L<sup>-1</sup> (from 0 to 432.9 μg L<sup>-1</sup>), respectively, and overall higher water level corresponded to lower Chl-a concentration (Fig. 4d-e). The temporal variations in these two factors were correlated since they were both regulated by pond water exchanges following the tidal rhythm. The timing of the daily peak water level (most in the afternoon) tended to postpone gradually within the semi-monthly spring-neap tidal cycles.

#### 3.2. Temporal variations in CO<sub>2</sub> flux

Temporal variations in (cumulative) NEE at daily and monthly scales over the aquaculture ponds from January 2020 to June 2022 were shown in Fig. 5. Over the study period, daily NEE ranged from -2.33-1.35 g CO<sub>2</sub>-C m<sup>-2</sup> day<sup>-1</sup> with the average of -0.48 g CO<sub>2</sub>-C m<sup>-2</sup> day<sup>-1</sup> (Fig. 5a). During the drainage period, daily NEE tended to change from a CO<sub>2</sub> sink to a CO<sub>2</sub> source. Temporal variations in monthly NEE indicated that algae-shellfish aquaculture ponds acted as a consistent daytime CO<sub>2</sub> sink and a weak nighttime CO<sub>2</sub> source (Fig. 5b). Monthly NEE varied from -32.8-0.50 g CO<sub>2</sub>-C m<sup>-2</sup> month<sup>-1</sup> with higher CO<sub>2</sub> sinks in spring. Monthly NEE showed different seasonal variations between daytime and nighttime, which varied from -36.7 to -11.8 g CO<sub>2</sub>-C m<sup>-2</sup> month<sup>-1</sup> and -4.7-23.4 g CO<sub>2</sub>-C m<sup>-2</sup> month<sup>-1</sup>, respectively. In contrast with consistent daytime CO<sub>2</sub> sinks through the year, the ponds at nighttime tended to act as a CO<sub>2</sub> source from April to December and turn into a neutral system from January to March.

The 30-min NEE over the aquaculture ponds fluctuated a lot with strong diurnal variations, and the 30-min values over the first three months of 2020 ranged from -9.27-8.98 μmol m<sup>-2</sup> s<sup>-1</sup> (Fig. 4a). Over the study period, the NEE shared a similar mean diurnal variation among seasons with strong daytime sinks and weak nighttime sources, where daytime sinks peaking at ~ 3 pm (Fig. 6). The ranges of mean

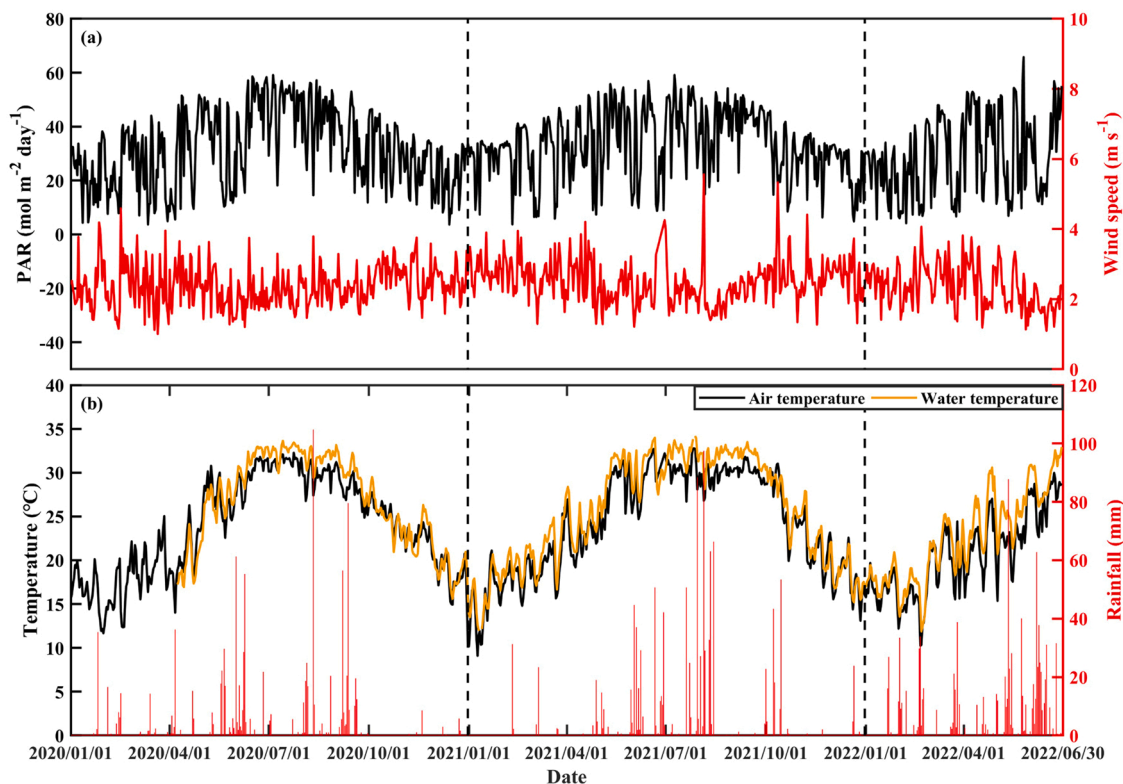


Fig. 2. Temporal variations in daily meteorological measurements from January 2020 to June 2022 including daily cumulative photosynthetically active radiation (PAR; black line), wind speed (red line), daily mean air (Ta, black line), water temperature (Tw, yellow line), and daily rainfall (red bar).

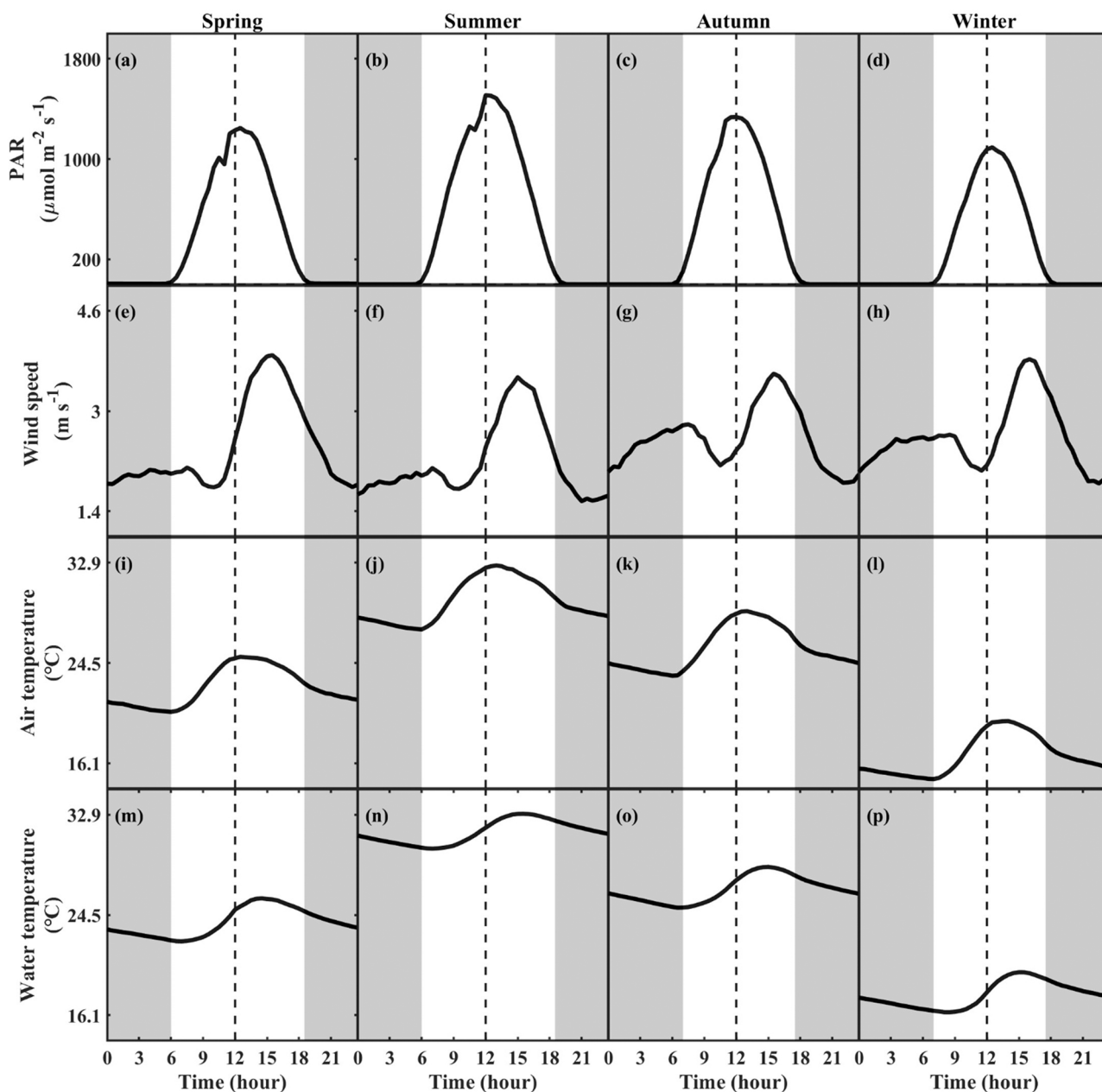


Fig. 3. Mean diurnal variations in (a-d) photosynthetically active radiation (PAR), (e-h) wind speed, (i-j) air temperature ( $T_a$ ), and (m-p) water temperature ( $T_w$ ) for each season from January 2020 to June 2022. Daytime and nighttime are indicated by white and gray areas.

diurnal variation differed across months and seasons: spring ( $-2.62$  to  $0.86 \mu\text{mol m}^{-2} \text{s}^{-1}$ ), summer ( $-2.89$  to  $1.77 \mu\text{mol m}^{-2} \text{s}^{-1}$ ), autumn ( $-2.02$  to  $1.19 \mu\text{mol m}^{-2} \text{s}^{-1}$ ), and winter ( $-1.72$  to  $0.50 \mu\text{mol m}^{-2} \text{s}^{-1}$ ). At daytime, the  $\text{CO}_2$  sink was stronger in summer ( $-1.87 \pm 2.16 \mu\text{mol m}^{-2} \text{s}^{-1}$ ) and spring ( $-1.60 \pm 2.09 \mu\text{mol m}^{-2} \text{s}^{-1}$ ) than in autumn ( $-1.21 \pm 1.79 \mu\text{mol m}^{-2} \text{s}^{-1}$ ) and winter ( $-1.14 \pm 1.54 \mu\text{mol m}^{-2} \text{s}^{-1}$ ). At nighttime, the  $\text{CO}_2$  source was stronger in summer ( $0.88 \pm 2.49 \mu\text{mol m}^{-2} \text{s}^{-1}$ ) and autumn ( $0.73 \pm 2.02 \mu\text{mol m}^{-2} \text{s}^{-1}$ ) than in spring ( $0.30 \pm 2.19 \mu\text{mol m}^{-2} \text{s}^{-1}$ ) and winter ( $0.13 \pm 1.59 \mu\text{mol m}^{-2} \text{s}^{-1}$ ).

The diurnal pattern of NEE during different farming periods varied greatly (Fig. 7). During the razor clam farming period, the ponds acted as a daytime sink and a weak nighttime source, ranging from  $-1.97$ – $0.59 \mu\text{mol m}^{-2} \text{s}^{-1}$  with a daily mean flux of  $-0.42 \mu\text{mol m}^{-2} \text{s}^{-1}$ . The late stage of the razor clam farming period had a stronger daytime sink and a weaker nighttime source in comparison with the early stage. The diurnal variation in the early and late razor clam farming periods ranged from  $-1.70$ – $1.12$  (average of  $-0.04$ )  $\mu\text{mol m}^{-2}$

$\text{s}^{-1}$  and from  $-2.23$ – $0.39$  (average of  $-0.63$ )  $\mu\text{mol m}^{-2} \text{s}^{-1}$ , respectively. In comparison with the razor clam farming period, NEE in the shrimp-crab farming period tended to be stronger daytime sinks and nighttime sources, varying from  $-2.89$ – $1.77 \mu\text{mol m}^{-2} \text{s}^{-1}$  (average of  $-0.50$ ). For the drainage period, NEE fluctuated from  $-2.95$ – $3.29 \mu\text{mol m}^{-2} \text{s}^{-1}$  with an average of  $0.40 \mu\text{mol m}^{-2} \text{s}^{-1}$ , showing the weakest daytime  $\text{CO}_2$  uptake and the strongest nighttime  $\text{CO}_2$  emissions among all periods.

### 3.3. Environmental controls on $\text{CO}_2$ flux

Pearson correlation analyses were conducted to explore the links between 30-min NEE and related environment variables (Table 1). For all day and daytime, the NEE was statistically ( $p < 0.05$ ) correlated with all of these seven environment variables, with PAR (correlation coefficients of  $-0.51$  and  $-0.44$  for all day and daytime, respectively), DO ( $-0.26$  and  $-0.28$ ), and  $T_a$  ( $-0.20$  and  $-0.26$ ) ranking the top three

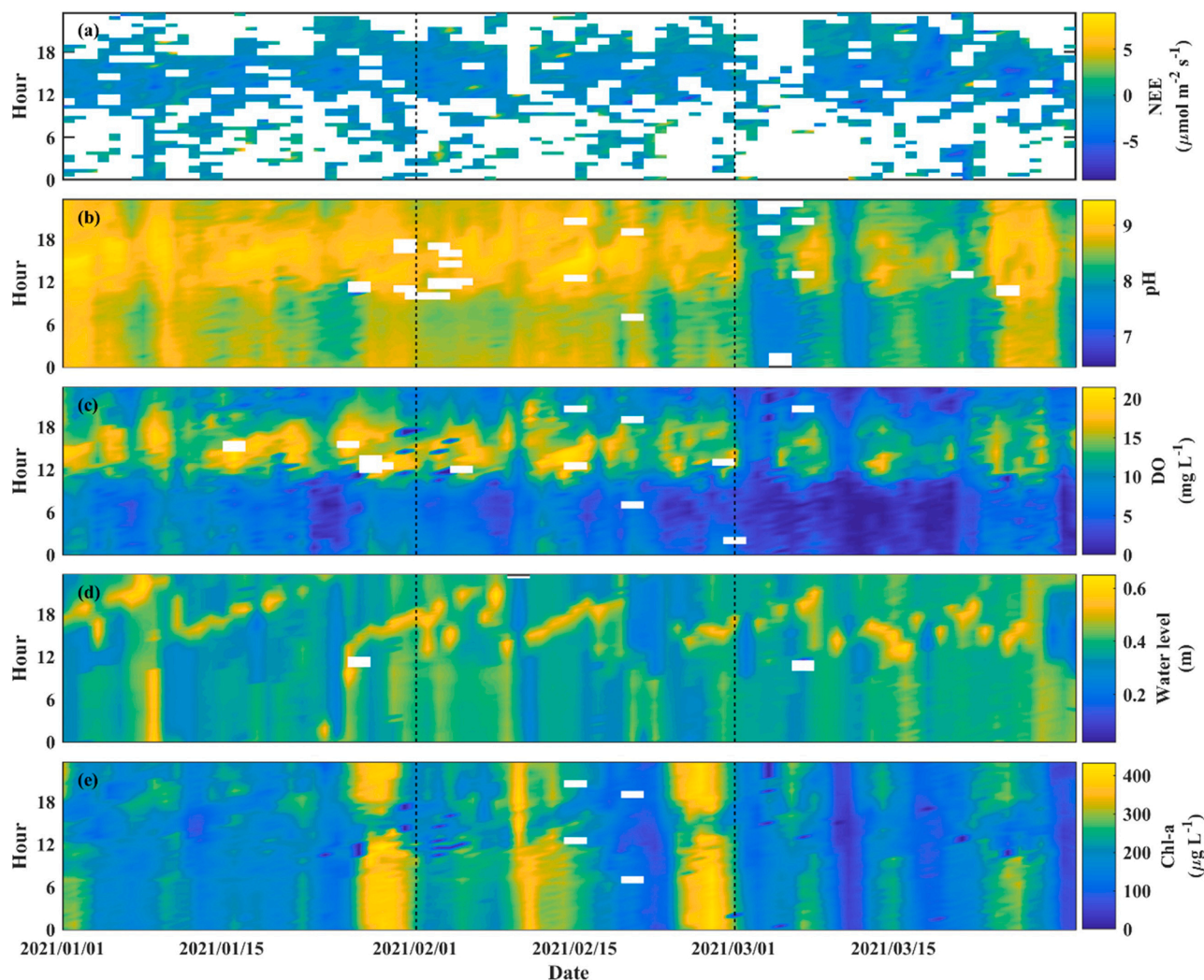


**Fig. 4.** Diurnal variations in 30-min measurements of (a) net ecosystem exchange (NEE), (b) pH, (c) dissolved oxygen (DO), (d) water level, and Chlorophyll a (Chl-a) from January to March 2021.

correlations. For nighttime, the NEE was statistically correlated with all but one environmental variable (Chl-a). The three most important controls on nighttime NEE were  $T_a$  (0.14),  $W_s$  (−0.11), and  $T_w$  (0.09), but their correlations were weaker than those for all day and daytime.

Over the study period, daily and monthly diurnal variability factors,  $V_{DN}$ , ranged from 0.0 to 4.0 (average of 1.4) and 0.8–2.0 (average of 1.3), respectively (Fig. 8a-b). Among the environmental variables, we found both daily and monthly  $V_{DN}$  were statistically ( $p < 0.05$ ) positively correlated with air temperature. The mean value of  $V_{DN}$  was estimated as 1.3 over the study period (1.2, 1.5, and 3.2 for algae-shellfish, shrimp-crab, and drainage periods, respectively), which was generally higher than those values of other studies covering various aquatic ecosystem types and flux measurement approaches (Fig. 8c). Taken all these values together, we found the  $V_{DN}$  tended to increase with decreasing latitudes. The diurnal correction factor,  $C_{DN}$ , based on the measurements over the study period was estimated as 0.41, 0.26, 0.20, 0.44, and 0.35 for spring, summer, autumn, winter, and all seasons, respectively. The  $C_{DN}$  was estimated as 0.40 (0.16/0.49), 0.26, and −0.62 for algae-shellfish (early/late stage), shrimp-crab, and drainage periods, respectively.

## 4. Discussion

### 4.1. Diurnal flux variability across months and seasons

High temporal variations of NEE have been found in numerous aquatic ecosystems including aquaculture ponds, lakes, rivers, and reservoirs (Gorsky et al., 2021; Lin et al., 2022; Ran et al., 2022; Tong et al., 2021). Our study found a clear diurnal pattern with a strong daytime  $CO_2$  sink and weak nighttime  $CO_2$  source over algae-shellfish aquaculture ponds, which was consistent with previous studies showing similar diurnal patterns in the coastal zone (Chien et al., 2018; Tong et al., 2013).

Some previous studies found that the strength of the daytime sources exceeded the nighttime sources (Hu et al., 2020; Martinez-Cruz et al., 2020; Van Dam et al., 2021), while others confirmed stronger nighttime sources (Reiman and Xu, 2019). However, the majority of previous studies focused on the diurnal variability of NEE in summer based on discontinuous flux measurements.

In this study, the diurnal NEE showed large fluctuations in all months, with summer and autumn showing stronger daytime  $CO_2$  sinks and nighttime  $CO_2$  sources compared to spring and winter. The difference in diurnal NEE pattern among seasons has been also found in river ecosystems (Reiman and Xu, 2019). The difference between daytime and nighttime fluxes was not consistent throughout the year in this study,

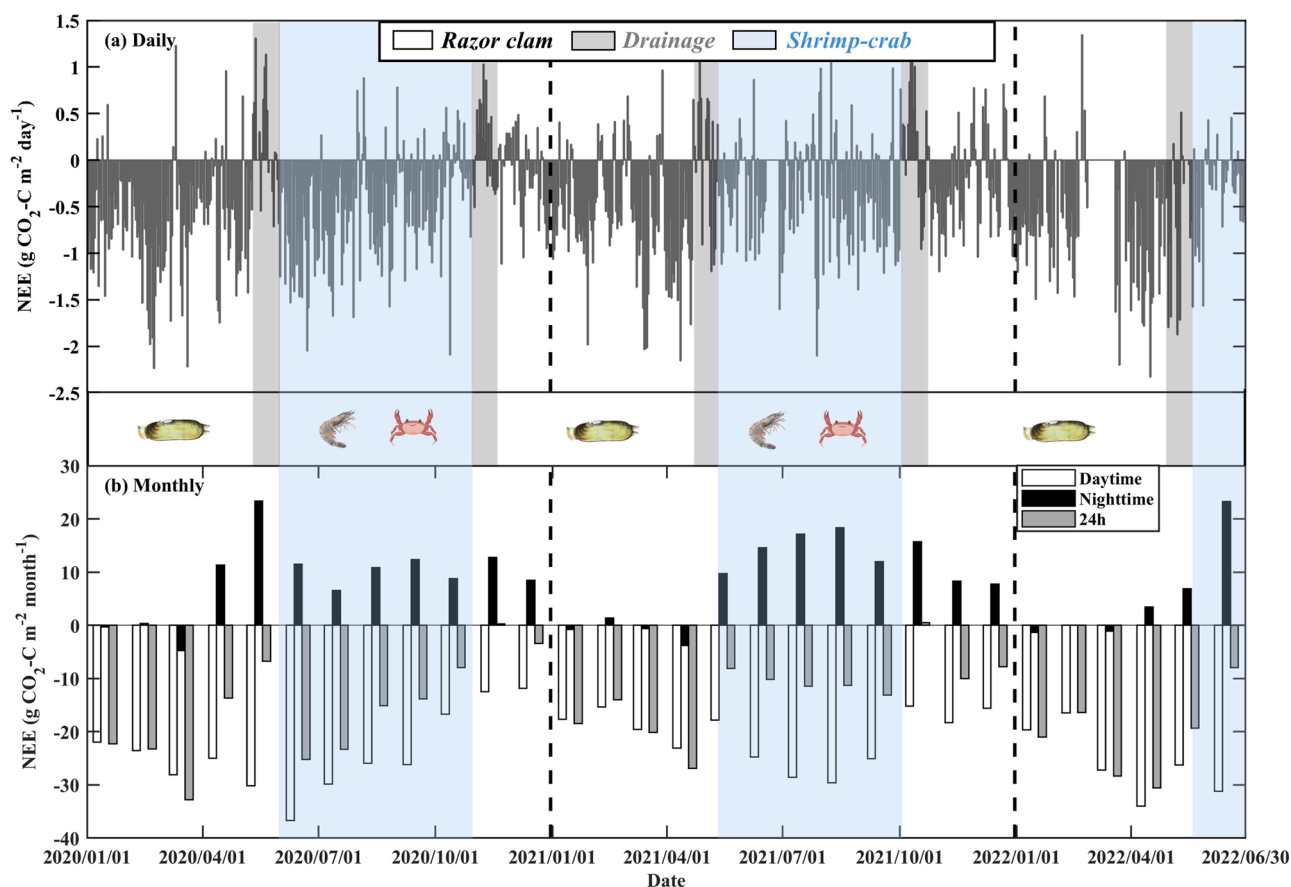


Fig. 5. Daily (a) and monthly (b) cumulative net ecosystem exchange (NEE) over aquaculture ponds from January 2020 to June 2022. Different farming (razor clam or shrimp-crab) or management (drainage) stages are marked and the monthly data for daytime and nighttime periods are also shown.

suggesting that the effect of diurnal variation on estimating carbon budgets should be assessed on a seasonal or even monthly basis.

#### 4.2. Diurnal flux variability across aquaculture managements

Aquaculture modes and farming species are the key factors to determine the carbon budget in aquaculture systems (Yuan et al., 2019; Zhang et al., 2022b). Previous studies have found that the NEE was significantly different between farming and non-farming periods (Tong et al., 2021). Different farming periods could have distinct diurnal patterns of NEE due to the difference in farming species and management, and the diurnal pattern with the same farming regime may also be affected by various methods or timings of flux measurements. This study confirmed that diurnal variation of NEE was different between razor clam farming stages (early and late) and among various farming/management periods including razor clam, shrimp-crab, and drainage.

It is noted that, at nighttime, the ponds acted as a CO<sub>2</sub> source during the early stage of the razor clam period but turned into a neutral or even CO<sub>2</sub> sink (Fig. 5b). This source-sink transition was consistently identified in three consecutive razor clam farming seasons over the study period. Given that the CO<sub>2</sub> sink can be enhanced by the calcification process with shellfish growth (Han et al., 2017; Jiang et al., 2015; Li et al., 2021), we speculate the phenomenon of nighttime neutral or CO<sub>2</sub> sink during the late stage of razor clam farming period may be associated with the calcification process along with the shell growth of razor clam. During the razor clam farming period, the mean CO<sub>2</sub> sink in the late stage was ~ 16 times of that in the early stage, which further suggested that, in addition to farming species, different farming stages also mattered in affecting NEE and its diurnal variations.

It is also known that pond management practices such as drainage could affect the temporal variability of NEE over aquaculture ponds (Kosten et al., 2020). In this study, we did identify a sink-source transition pattern in NEE from the farming to the drainage period (Fig. 5a), which was also reported in another study on aquaculture ponds (Yang et al., 2018a). This sink-source transition could be explained by the combination of reduced photosynthetic carbon uptake by algae due to drainage and enhanced respiratory carbon emissions due to extended exposure of pond sediments to the air.

#### 4.3. Effects of environmental factors

The CO<sub>2</sub> uptake was associated with the photosynthesis of planktonic algae and the emissions was associated with ecosystem respiration (Demars et al., 2016; Jammot et al., 2017). The diurnal variations in NEE over algae-shellfish aquaculture ponds in this study could be explained by the fact that daytime NEE was dominated by algae photosynthesis while nighttime NEE was significantly affected by ecosystem respiration (Ye et al., 2022; Zhang et al., 2022a). As shown by the correlation analyses, environmental controls on daytime and nighttime NEE were not the same, where daytime and nighttime NEE were most regulated by PAR and air temperature, respectively.

PAR or air temperature is not the only factor affecting the diurnal variations in NEE. For example, in the daytime, both NEE and PAR had single-peak diurnal patterns, but the timings of their peaks were different, where the peak of NEE was ~ 3 h lagged behind PAR peaking at noon (Figs. 3 and 6). In addition to PAR, the temperature may regulate NEE in different ways including affecting microbial activities, redox environment, and gas solubility in water (Van Dam et al., 2021; Yang et al., 2018b). The important role of temperature in driving diurnal

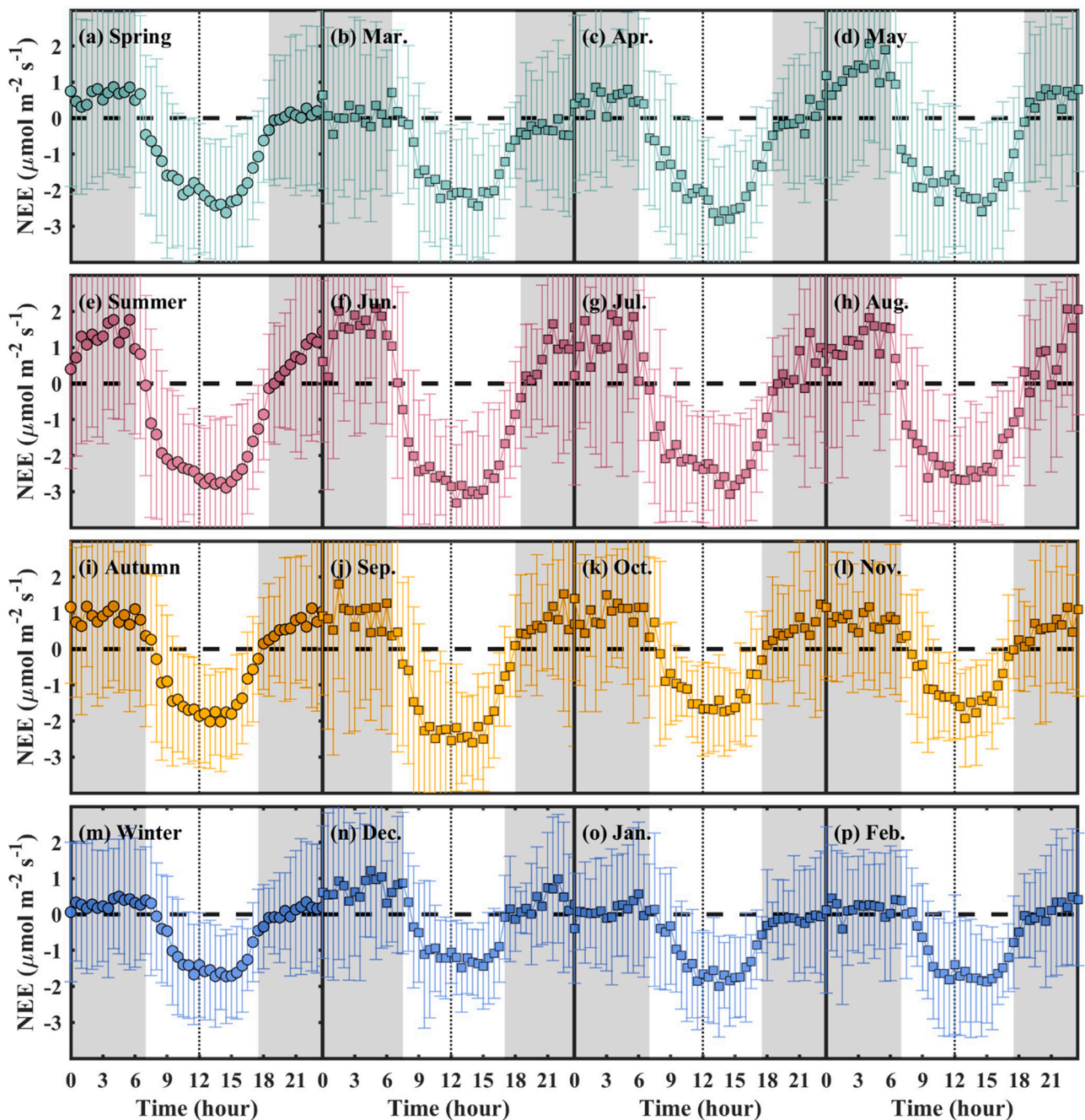


Fig. 6. Mean diurnal variations in net ecosystem exchange (NEE) over aquaculture ponds for each season and month from January 2020 to June 2022. Standard error of multi-day NEE values for each 30-min are also shown. Daytime and nighttime are indicated by white and gray areas.

variations in NEE has been confirmed in many previous studies examining the  $\text{CO}_2$  flux across the water-air interface in aquatic ecosystems (Li et al., 2018; Xu et al., 2019).

As for water quality factors, the NEE over these aquaculture ponds was negatively correlated with pH and DO, which was consistent with other studies (Gruca-Rokosz et al., 2017; Xiao et al., 2020; Zhang et al., 2022a). Previous studies also found a negative correlation between NEE and Chl-a concentration (Xiao et al., 2020; Yu et al., 2022), but this correlation was not identified in this study. It was not surprising, however, since Chl-a concentration in the pond with frequent water exchanges might be more regulated by the amount of pond water than the growth of algae.

#### 4.4. Implication on carbon budget estimations

The positive effect of air temperature on  $V_{\text{DN}}$  identified in this study was also found in previous studies on aquatic ecosystems (Attemeyer et al., 2021; Rudberg et al., 2021). Compare with other aquatic ecosystems, the algae-shellfish aquaculture ponds had stronger diurnal NEE variation with higher  $V_{\text{DN}}$  averaged over all periods (Fig. 8c). On the one hand, the stronger diurnal variability could be explained by the fact that the aquaculture ponds in this study were much richer in algae compared to other aquatic ecosystems. On the other hand, the difference among ecosystems was also associated with different flux measuring approaches and timings. For example, the EC-based NEE observed in this study was significantly different from the chamber-based NEE over algae-shellfish aquaculture ponds at a similar latitude (Ye et al., 2022).



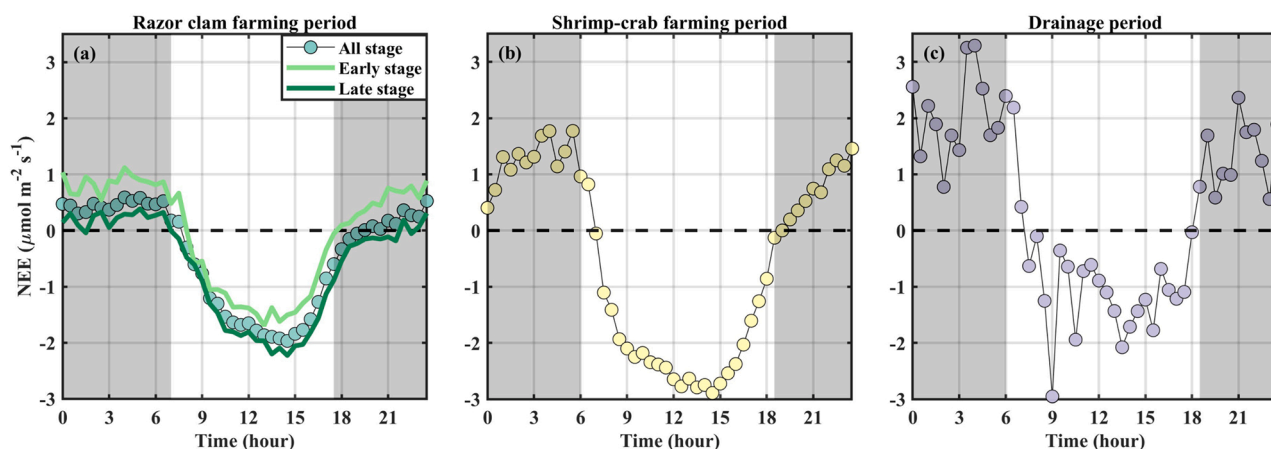


Fig. 7. Mean diurnal variations in net ecosystem exchange (NEE) over aquaculture ponds during different farming or management periods including (a) razor clam farming (early, late, and all stages), (b) shrimp-crab farming, and (c) drainage. Daytime and nighttime are indicated by white and gray areas.

Table 1

Pearson correlation coefficients ( $r$ ) among 30-min time series of net ecosystem  $\text{CO}_2$  exchange (NEE) and related environmental variables including wind speed (Ws), photosynthetically active radiation (PAR), air temperature (Ta), water temperature (Tw), pH, dissolved oxygen (DO), and Chlorophyll a (Chl-a). The correlation analyses were also conducted for daytime and nighttime NEE. Note the data of NEE, Ws, PAR, and Ta were available from January 2020 to June 2022, while the rest variables were only available from January to March 2021. All values shown are statistically significant at  $p < 0.05$ , and the top three correlation coefficients are marked in bold for all day, daytime, and nighttime NEE.

$r$	NEE			Ws	PAR	Ta	Tw	pH	DO
	All	Daytime	Nighttime						
Ws	-0.18	-0.11	<b>-0.11</b>						
PAR	<b>-0.51</b>	<b>-0.44</b>	-0.07	0.17					
Ta	<b>-0.20</b>	<b>-0.26</b>	<b>0.14</b>	-0.07	0.46				
Tw	-0.13	-0.22	<b>0.09</b>	-0.05	0.27	0.93			
Ph	-0.11	-0.14	-0.06	0.23	0.16		-0.09		
DO	<b>-0.26</b>	<b>-0.28</b>	-0.08	0.36	0.45	0.15		0.58	
Chl-a	0.09	0.11		-0.05	-0.20	-0.23	-0.23	0.24	0.21

The higher  $V_{DN}$  observed in this study highlighted the importance of considering the diurnal variability in assessing the carbon budgets of algae-shellfish aquaculture ponds. The increasing trend of  $V_{DN}$  with decreasing latitude implied that the NEE over aquatic ecosystems was likely to have stronger diurnal variations at lower latitudes (or perhaps warmer temperatures).

All the values of  $C_{DN}$  during various periods were lower than one, suggesting that the estimates based on daytime-only flux measurements would overestimate  $\text{CO}_2$  uptake during algae-shellfish and shrimp-crab farming periods and even incorrectly shift a source into a sink during the drainage period. In fact, for algae-shellfish aquaculture ponds, the mean NEE over the day was only about one-third of the mean daytime NEE, implying that previous estimates without down-scaling corrections of daytime flux measurements could obviously bias the actual carbon budgets.

#### 4.5. Limitation and outlook

The field measurements and data analyses of this study suffered from several limitations and uncertainties. First, although high-frequency EC measurements can well capture the diurnal variability of NEE over aquaculture ponds, these EC-based  $\text{CO}_2$  fluxes could be biased due to imperfect flux correction and quality control processes. To reduce this uncertainty, in this study we only focused on mean diurnal variations in NEE instead of individual days. This was statistically reasonable since 30-min NEE usually fluctuated a lot over any single day and thus it was almost impossible to accurately attribute the diurnal variability of NEE to any specific management activity observed within the day.

Second, the EC-based NEE represented net ecosystem  $\text{CO}_2$  exchanges

over a spatial coverage of tens of ponds ( $\sim 400$  m around the tower for the 90% footprint climatology), we were not able to partition the contribution of NEE from different types of ponds (e.g., algae vs. razor clam) or various flux components (e.g., calcification-induced flux). Future studies combining other flux measuring approaches such as floating chamber (Shahan et al., 2022) and boundary layer models (Erkkila et al., 2018) are needed to improve the understanding of the heterogeneity of NEE and its environmental controls at finer spatial scales.

Third, for an inhomogeneous flux footprint as in this study, the difference in diurnal flux variability among various periods (i.e., seasons, farming species, and drainage) could be also affected by inconsistent footprint climatology across these periods. It was difficult to accurately quantify this footprint-related effect due to the lack of the information on aquaculture management and flux variability for each pond within the footprint. However, our further footprint analyses individually for each period (Fig. S1) confirmed that the footprint-weighted area proportion of algae ponds within the 90% footprint area for each period varied little (0.43  $\sim$  0.46), which suggested that the varying footprint might play a small role in affecting the diurnal flux variability.

Finally, the EC-based NEE in this study only represented the diurnal pattern of  $\text{CO}_2$  flux over algae-shellfish aquaculture ponds with dominant farming species of razor clam, but, for a comprehensive assessment of NEE over aquaculture ponds, more empirical studies are needed to cover aquaculture ponds with other farming species and management practices (Yang et al., 2022).

Recent synthesis studies on the GHG fluxes of aquaculture ponds (Yuan et al., 2019; Zhang et al., 2022b) have emphasized the differences in flux direction, magnitude, and their environmental or anthropogenic

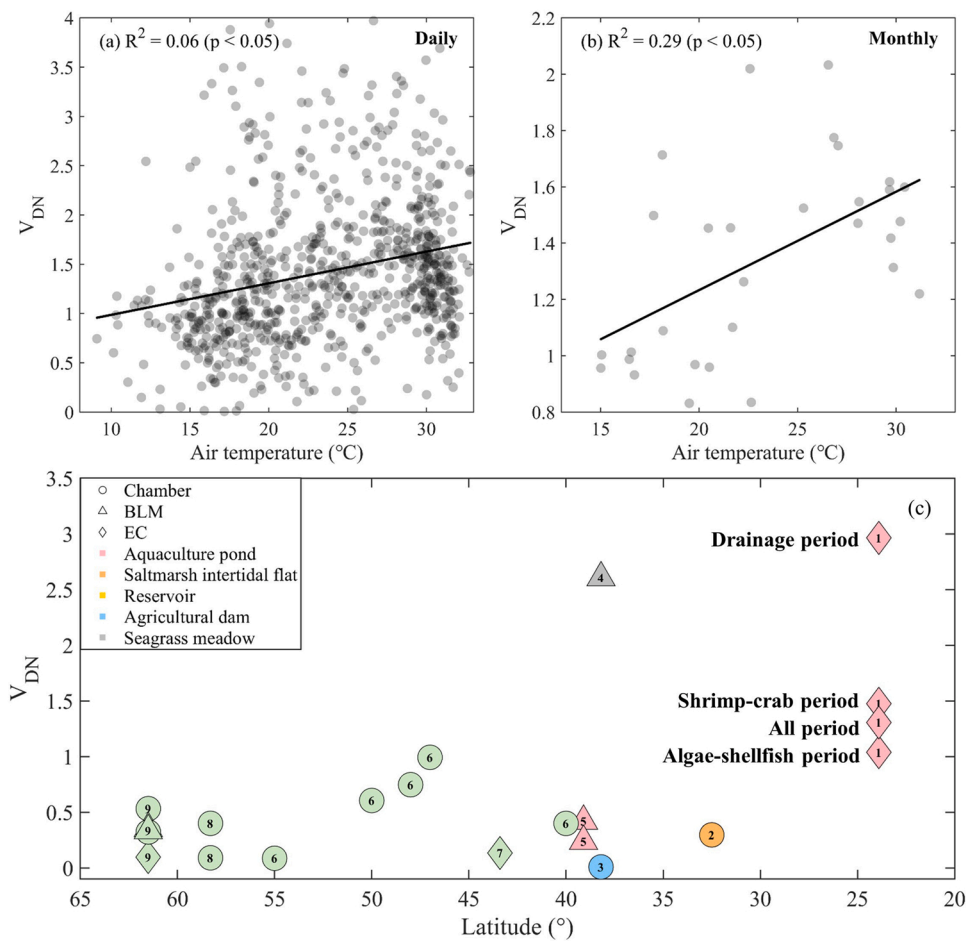


**Fig. 8.** The diurnal variability factor of  $V_{DN}$  (defined as the absolute value of the ratio of the difference between daytime and nighttime NEE (net ecosystem  $\text{CO}_2$  exchange) over daytime NEE) as a function of air temperature at daily (a) and monthly (b) time scales with corresponding linear fitting lines. The values of  $V_{DN}$  for the aquaculture ponds of this study and other aquatic ecosystems are shown along with decreasing latitudes (c). The values are marked with various colors and symbols, respectively, indicating different ecosystem types and flux measuring approaches, including chamber, boundary layer models (BLM), and eddy covariance (EC).

The number on each marker denotes the source reference: (1) this study, (2) Xu et al. (2017), (3) Ollivier et al. (2019), (4) Ollivier et al. (2022), (5) Hu et al. (2020), (6) Attermeyer et al. (2021), (7) Czikowsky et al. (2018), (8) Rudberg et al. (2021), and (9) Erkkila et al. (2018). (b) See more information on the source reference and related data in Table S1.

controls among various farming species and practices. The findings from this EC-based case study did echo this statement, however, we also emphasized the necessity of future studies to cover under-represented aquaculture ponds like razor clam, which experienced unique flux variation patterns. Another recent study (Kosten et al., 2020) highlighted the importance to consider the temporal variations (especially at diurnal scale) of these fluxes in assessing carbon budgets. As evident in this study, the diurnal variability often outweighed the variation ranges across farming/management periods.

Given that the diurnal flux variability was rarely reported in aquaculture ponds (Kosten et al., 2020) due to the limit of traditional snapshot measurements, the findings of this study added an important piece of evidence to the diurnal flux variability over algae-shellfish aquaculture ponds. Future studies should pay more attention to the diurnal flux variability over various aquaculture systems and farming periods, which is critical to catching potential flux “hot-moments” with natural and human disturbances (e.g., the source-sink transition of flux occurring during the drainage) and improving the temporal aggregation from snapshot measurements.

## 5. Conclusions

The eddy covariance (EC) measurements of net ecosystem  $\text{CO}_2$  exchange (NEE) over algae-shellfish aquaculture ponds in Zhangjiang Estuary of Southeast China were conducted in this study to examine the diurnal variability of NEE across the water-air interface of the ponds under various farming/management periods. These EC flux measurements over the study period from January 2020 to June 2022 confirmed that algae-shellfish aquaculture ponds had strong diurnal variations in NEE with daytime sink and nighttime source, mainly controlled by PAR

and air temperature, respectively. The ponds acted as a net sink system during razor clam and shrimp-crab farming periods experiencing stronger daytime sink than the nighttime source, while it was the opposite during the drainage period acting as a net source. The strength of sink/source also differed between the early and late stages of the razor clam farming period, with much larger net carbon uptake in the late stage as a result of strong daytime sink and near-neutral nighttime flux. The diurnal variability of NEE over the ponds was overall larger than other aquatic ecosystems and tended to increase with air temperature. Previous estimates of daily NEE from discrete daytime-only samplings might have biased the actual carbon budgets if no diurnal correction was applied in the temporal aggregation. The strong temporal variability of NEE across diurnal and seasonal time scales highlighted the importance and necessity of continuous and high-frequency flux measurements in assessing the carbon budgets of algae-shellfish aquaculture ponds.

## Declaration of Competing Interest

The authors declare that they have no known competing financial interests or personal relationships that could have appeared to influence the work reported in this paper.

## Data Availability

Data will be made available on request.

## Acknowledgments

We are grateful to members of Coastal Ecology & Remote Sensing lab led by Dr. Xudong Zhu at Xiamen University and staff at Zhangjiang

Estuary Mangrove National Nature Reserve for their help in the fieldwork. This research was funded by the National Key Research and Development Program of China (2022YFF0802101), the Special Project on National Science and Technology Basic Resources Investigation of China (2021FY100704), the State Key Laboratory of Marine Environmental Science, Ministry of Science and Technology, China (MELRI2201), the Key Program of Marine Economy Development Special Foundation of Department of Natural Resources of Guangdong Province (GDNRC[2022]20), the Natural Science Foundation of Fujian Province, China (2020J01049), the Youth Innovation Foundation of Xiamen, China (3502Z20206038), and the Fundamental Research Funds for the Central Universities of China (20720210075).

## Appendix A. Supporting information

Supplementary data associated with this article can be found in the online version at [doi:10.1016/j.agee.2023.108426](https://doi.org/10.1016/j.agee.2023.108426).

## References

- Alonso, A.A., Álvarez-Salgado, X.A., Antelo, L.T., 2021. Assessing the impact of bivalve aquaculture on the carbon circular economy. *J. Clean. Prod.* 279. <https://doi.org/10.1016/j.jclepro.2020.123873>.
- Attermeyer, K., Casas-Ruiz, J.P., Fuss, T., Pastor, A., Cuvy-Fraunie, S., Sheath, D., et al., 2021. Carbon dioxide fluxes increase from day to night across European streams. *Commun. Earth Environ.* 2. <https://doi.org/10.1038/s43247-021-00192-w>.
- Baldocchi, A.K., Reed, D.E., Loken, L.C., Stanley, E.H., Huerd, H., Desai, A.R., 2020a. Comparing spatial and temporal variation of lake-atmosphere carbon dioxide fluxes using multiple methods. *J. Geophys. Res.: Biogeosciences* 125. <https://doi.org/10.1029/2019jg005623>.
- Baldocchi, D.D., 2020b. How eddy covariance flux measurements have contributed to our understanding of Global Change Biology. *Glob. Change Biol.* 26, 242–260. <https://doi.org/10.1111/gcb.14807>.
- Chen, Y., Dong, S.L., Wang, Z.N., Wang, F., Gao, Q.F., Tian, X.L., et al., 2016. Variations in CO<sub>2</sub> fluxes from grass carp *Ctenopharyngodon idella* aquaculture polyculture ponds. *Aquac. Environ. Interact.* 8, 31–40. <https://doi.org/10.3354/aei00149>.
- Chien, H., Zhong, Y.Z., Yang, K.H., Cheng, H.Y., 2018. Diurnal variability of CO<sub>2</sub> flux at coastal zone of Taiwan based on eddy covariance observation. *Cont. Shelf Res.* 162, 27–38. <https://doi.org/10.1016/j.csr.2018.04.006>.
- Czikowsky, M.J., MacIntyre, S., Tedford, E.W., Vidal, J., Miller, S.D., 2018. Effects of wind and buoyancy on carbon dioxide distribution and air-water flux of a stratified temperate lake. *J. Geophys. Res.: Biogeosciences* 123, 2305–2322. <https://doi.org/10.1029/2017jg004209>.
- David, F.S., Proenca, D.C., Flickinger, D.L., Bueno, G.W., Valenti, W.C., 2021. Carbon budget in integrated aquaculture systems with Nile tilapia (*Oreochromis niloticus*) and Amazon river prawn (*Macrobrachium amazonicum*). *Aquac. Res.* 52, 5155–5167. <https://doi.org/10.1111/are.15384>.
- Demars, B.O.L., Gislason, G.M., Olafsson, J.S., Manson, J.R., Friberg, N., Hood, J.M., et al., 2016. Impact of warming on CO<sub>2</sub> emissions from streams countered by aquatic photosynthesis. *Nat. Geosci.* 9, 758. <https://doi.org/10.1038/ngeo2807>.
- Dong, S.P., Wang, F., Zhang, D.X., Yu, L.Y., Pu, W.J., Shang, Y.K., 2022. Growth performance and ecological services evaluation of razor clams based on dynamic energy budget model. *J. Environ. Manag.* 306, 8. <https://doi.org/10.1016/j.jenvman.2021.114392>.
- Erkkila, K.M., Ojala, A., Bastviken, D., Biermann, T., Heiskanen, J.J., Lindroth, A., et al., 2018. Methane and carbon dioxide fluxes over a lake: comparison between eddy covariance, floating chambers and boundary layer method. *Biogeosciences* 15, 429–445. <https://doi.org/10.5194/bg-15-429-2018>.
- Fang, X.T., Wang, C., Zhang, T.R., Zheng, F.W., Zhao, J.T., Wu, S., et al., 2022a. Ebulitive CH<sub>4</sub> flux and its mitigation potential by aeration in freshwater aquaculture: measurements and global data synthesis. *Agric. Ecosyst. Environ.* 335. <https://doi.org/10.1016/j.agee.2022.108016>.
- Fang, X.T., Zhao, J.T., Wu, S., Yu, K., Huang, J., Ding, Y., et al., 2022b. A two-year measurement of methane and nitrous oxide emissions from freshwater aquaculture ponds: affected by aquaculture species, stocking and water management. *Sci. Total Environ.* 813. <https://doi.org/10.1016/j.scitotenv.2021.151863>.
- FAO, 2019. *State World Fish. Aquac.* 2016.
- Fisheries Department of Agriculture Ministry of China, 2021. *China Fishery Statistical Yearbook 2021*. Chinese Agriculture Press, Beijing.
- Friedlingstein, P., O'Sullivan, M., Jones, M.W., Andrew, R.M., Hauck, J., Olsen, A., et al., 2020. Global carbon budget 2020. *Earth Syst. Sci. Data* 12, 3269–3340. <https://doi.org/10.5194/essd-12-3269-2020>.
- Gomez-Gener, L., Rocher-Ros, G., Battin, T., Cohen, M.J., Dalmagro, H.J., Dinsmore, K.J., et al., 2021. Global carbon dioxide efflux from rivers enhanced by high nocturnal emissions. *Nat. Geosci.* 14, 289–294. <https://doi.org/10.1038/s41561-021-00722-3>.
- Gorsky, A.L., Lottig, N.R., Stoy, P.C., Desai, A.R., Dugan, H.A., 2021. The importance of spring mixing in evaluating carbon dioxide and methane flux from a small north-temperate lake in Wisconsin, United States. *J. Geophys. Res.: Biogeosciences* 126. <https://doi.org/10.1029/2021jg006537>.
- Gruca-Rokosz, R., Bartoszek, L., Koszelnik, P., 2017. The influence of environmental factors on the carbon dioxide flux across the water-air interface of reservoirs in south-eastern Poland. *J. Environ. Sci.* 56, 290–299. <https://doi.org/10.1016/j.jes.2016.10.011>.
- Han, T.T., Shi, R.J., Qi, Z.H., Huang, H.H., Liang, Q.Y., Liu, H.X., 2017. Interactive effects of oyster and seaweed on seawater dissolved inorganic carbon systems: implications for integrated multi-trophic aquaculture. *Aquac. Environ. Interact.* 9, 469–478. <https://doi.org/10.3354/aei00246>.
- Hu, B.B., Xu, X.F., Zhang, J.F., Wang, T.L., Meng, W.Q., Wang, D.Q., 2020. Diurnal variations of greenhouse gases emissions from reclamation mariculture ponds. *Estuar. Coast. Shelf Sci.* 237. <https://doi.org/10.1016/j.ecss.2020.106677>.
- Jammet, M., Dengel, S., Kettner, E., Parmentier, F.J.W., Wik, M., Crill, P., et al., 2017. Year-round CH<sub>4</sub> and CO<sub>2</sub> flux dynamics in two contrasting freshwater ecosystems of the subarctic. *Biogeosciences* 14, 5189–5216. <https://doi.org/10.5194/bg-14-5189-2017>.
- IPCC, 2023. *Summary for Policymakers*. In: Masson-Delmotte, V., Zhai, P., Pirani, A., Connors, S.L., Péan, C., Berger, S., Caud, N., Chen, Y., Goldfarb, L., Gomis, M.I., Huang, M., Leitzell, K., Lonnoy, E., Matthews, J.B.R., Maycock, T.K., Waterfield, T., Yelekli, O., Yu, R., Zhou, B. (Eds.), *Climate Change 2021: The Physical Science Basis. Contribution of Working Group I to the Sixth Assessment Report of the Intergovernmental Panel on Climate Change*. Cambridge University Press (In Press).
- Jiang, Z.J., Li, J.Q., Qiao, X.D., Wang, G.H., Bian, D.P., Jiang, X., et al., 2015. The budget of dissolved inorganic carbon in the shellfish and seaweed integrated mariculture area of Sanggou Bay, Shandong, China. *Aquaculture* 446, 167–174. <https://doi.org/10.1016/j.aquaculture.2014.12.043>.
- Kormann, R., Meixner, F.X., 2001. An analytical footprint model for non-neutral stratification. *Bound.-Layer. Meteorol.* 99, 207–224. <https://doi.org/10.1023/a:1018991015119>.
- Kosten, S., Almeida, R.M., Barbosa, I., Mendonça, R., Santos Muzitano, I., Sobreira Oliveira-Junior, E., et al., 2020. Better assessments of greenhouse gas emissions from global fish ponds needed to adequately evaluate aquaculture footprint. *Sci. Total Environ.* 748. <https://doi.org/10.1016/j.scitotenv.2020.141247>.
- Li, J.Q., Zhang, W.W., Ding, J.K., Xue, S.Y., Huo, E., Ma, Z.F., et al., 2021. Effect of large-scale kelp and bivalve farming on seawater carbonate system variations in the semi-enclosed Sanggou Bay. *Sci. Total Environ.* 753, 142065. <https://doi.org/10.1016/j.scitotenv.2021.142065>.
- Li, S.Y., Bush, R.T., Santos, I.R., Zhang, Q.F., Song, K.S., Mao, R., et al., 2018. Large greenhouse gases emissions from China's lakes and reservoirs. *Water Res.* 147, 13–24. <https://doi.org/10.1016/j.watres.2018.09.053>.
- Lin, Q.W., Wang, S.S., Li, Y.C., Riaz, L., Yu, F., Yang, Q.X., et al., 2022. Effects and mechanisms of land-types conversion on greenhouse gas emissions in the Yellow River floodplain wetland. *Sci. Total Environ.* 813. <https://doi.org/10.1016/j.scitotenv.2021.152406>.
- Liu, Y., Zhang, J.H., Wu, W.G., Zhong, Y., Li, H.M., Wang, X.M., et al., 2022. Effects of shellfish and macro-algae IMTA in North China on the environment, inorganic carbon system, organic carbon system, and sea-air CO<sub>2</sub> fluxes. *Front. Mar. Sci.* 9. <https://doi.org/10.3389/fmars.2022.864306>.
- Martinez-Cruz, K., Sepulveda-Jauregui, A., Greene, S., Fuchs, A., Rodriguez, M., Pansch, N., et al., 2020. Diel variation of CH<sub>4</sub> and CO<sub>2</sub> dynamics in two contrasting temperate lakes. *Inland Waters* 10, 333–347. <https://doi.org/10.1080/20442041.2020.1728178>.
- Mauder, M., Cuntz, M., Drié, C., Graf, A., Rebmann, C., Schmid, H.P., et al., 2013. A strategy for quality and uncertainty assessment of long-term eddy-covariance measurements. *Agric. For. Meteorol.* 169, 122–135. <https://doi.org/10.1016/j.agrformet.2012.09.006>.
- Morin, T.H., Riley, W.J., Grant, R.F., Mekonnen, Z., Stefanik, K.C., Sanchez, A.C.R., et al., 2022. Water level changes in Lake Erie drive 21st century CO<sub>2</sub> and CH<sub>4</sub> fluxes from a coastal temperate wetland. *Sci. Total Environ.* 821, 153087. <https://doi.org/10.1016/j.scitotenv.2022.153087>.
- Ollivier, Q.R., Maher, D.T., Pitfield, C., Macreadie, P.I., 2019. Winter emissions of CO<sub>2</sub>, CH<sub>4</sub>, and N<sub>2</sub>O from temperate agricultural dams: fluxes, sources, and processes. *Ecosphere* 10. <https://doi.org/10.1002/ecs2.2914>.
- Ollivier, Q.R., Maher, D.T., Pitfield, C., Macreadie, P.I., 2022. Net drawdown of Greenhouse Gases (CO<sub>2</sub>, CH<sub>4</sub> and N<sub>2</sub>O) by a temperate Australian seagrass meadow. *Estuaries Coasts*. <https://doi.org/10.1007/s12237-022-01068-8>.
- Pu, Y.N., Zhang, M., Jia, L., Zhang, Z., Xiao, W., Liu, S.D., et al., 2022. Methane emission of a lake aquaculture farm and its response to ecological restoration. *Agric., Ecosyst. Environ.* 330, 107883. <https://doi.org/10.1016/j.agee.2022.107883>.
- Ran, L.S., Yue, R., Shi, H.Y., Meng, X.D., Fang, N.F., Shi, Z.H., et al., 2022. Seasonal and diel variability of CO<sub>2</sub> emissions from a semiarid hard-water reservoir. *J. Hydrol.* 608. <https://doi.org/10.1016/j.jhydrol.2022.127652>.
- Reiman, J.H., Xu, Y.J., 2019. Diel variability of pCO<sub>2</sub> and CO<sub>2</sub> outgassing from the lower Mississippi River: Implications for riverine CO<sub>2</sub> outgassing estimation. *Water* 11. <https://doi.org/10.3390/w11010043>.
- Ren, C.Y., Wang, Z.M., Zhang, Y.Z., Zhang, B., Chen, L., Xi, Y.B., et al., 2019. Rapid expansion of coastal aquaculture ponds in China from Landsat observations during 1984–2016. *Int. J. Appl. Earth Obs. Geoinf.* 82, 12. <https://doi.org/10.1016/j.jag.2019.101902>.
- Ren, W.H., 2021. Study on the removable carbon sink estimation and decomposition of influencing factors of mariculture shellfish and algae in China: a two-dimensional perspective based on scale and structure. *Environ. Sci. Pollut. Res.* 28, 21528–21539. <https://doi.org/10.1007/s11356-020-11997-1>.
- Rudberg, D., Duc, N.T., Schenk, J., Sieczko, A.K., Pajala, G., Sawakuchi, H.O., et al., 2021. Diel Variability of CO<sub>2</sub> Emissions From Northern Lakes. *J. Geophys. Res.: Biogeosciences* 126. <https://doi.org/10.1029/2021jg006246>.

- Shahan, J., Chu, H.S., Windham-Myers, L., Matsumura, M., Carlin, J., Eichelmann, E., et al., 2022. Combining eddy covariance and chamber methods to better constrain CO<sub>2</sub> and CH<sub>4</sub> fluxes across a heterogeneous restored tidal wetland. *J. Geophys. Res.-Biogeosciences* 127. <https://doi.org/10.1029/2022jg007112>.
- Sieczko A.K., Duc N.T., Schenk J., Pajala G., Rudberg D., Sawakuchi H.O., et al. 2020. Diel variability of methane emissions from lakes. *Proceedings of the National Academy of Sciences of the United States of America*. 117: 21488–21494. <https://doi.org/10.1073/pnas.2006024117>.
- Tong, C., Huang, J.F., Hu, Z.Q., Jin, Y.F., 2013. Diurnal variations of carbon dioxide, methane, and nitrous oxide vertical fluxes in a subtropical estuarine marsh on neap and spring tide days. *Estuaries Coasts* 36, 633–642. <https://doi.org/10.1007/s12237-013-9596-1>.
- Tong, C., Bastviken, D., Tang, K.W., Yang, P., Yang, H., Zhang, Y.F., et al., 2021. Annual CO<sub>2</sub> and CH<sub>4</sub> fluxes in coastal earthen ponds with *Litopenaeus vannamei* in southeastern China. *Aquaculture* 545, 10. <https://doi.org/10.1016/j.aquaculture.2021.737229>.
- Tranvik, L.J., Downing, J.A., Cotner, J.B., Loiselle, S.A., Striegl, R.G., Ballatore, T.J., et al., 2009. Lakes and reservoirs as regulators of carbon cycling and climate. *Limnol. Oceanogr.* 54, 2298–2314. <https://doi.org/10.4319/lo.2009.54.6.part.2.2298>.
- Van Dam, B.R., Lopes, C.C., Polsenaere, P., Price, R.M., Rutgersson, A., Fourqurean, J.W., 2021. Water temperature control on CO<sub>2</sub> flux and evaporation over a subtropical seagrass meadow revealed by atmospheric eddy covariance. *Limnol. Oceanogr.* 66, 510–527. <https://doi.org/10.1002/lno.11620>.
- Wu, Q.C., Fang, B.Z., Lin, W.S., Huang, G.M., Wang, M., 2012. Yield and value of fishery products of Zhangjiangkou mangrove forestry national nature reserve. *Weil. Sci. Manag.* 8, 34–38. <https://doi.org/10.3969/j.issn.1673-3290.2012.01.10>.
- Xiao, Q.T., Zhang, M., Hu, Z.H., Gao, Y.Q., Hu, C., Liu, C., et al., 2017. Spatial variations of methane emission in a large shallow eutrophic lake in subtropical climate. *J. Geophys. Res.-Biogeosciences* 122, 1597–1614. <https://doi.org/10.1002/2017jg003805>.
- Xiao, Q.T., Xu, X.F., Duan, H.T., Qi, T.C., Qin, B.Q., Lee, X., et al., 2020. Eutrophic Lake Taihu as a significant CO<sub>2</sub> source during 2000–2015. *Water Res.* 170. <https://doi.org/10.1016/j.watres.2019.115331>.
- Xiao, Q.T., Hu, Z.H., Hu, C., Islam, A.R.M.T., Bian, H., Chen, S.T., et al., 2021. A highly agricultural river network in Jurong Reservoir watershed as significant CO<sub>2</sub> and CH<sub>4</sub> sources. *Sci. Total Environ.* 769, 144558 <https://doi.org/10.1016/j.scitotenv.2020.144558>.
- Xu, C.J., Su, G.H., Zhao, K.S., Xu, X.Q., Li, Z.Q., Hu, Q., et al., 2022. Current status of greenhouse gas emissions from aquaculture in China. *Water Biol. Secur.* 1, 100041 <https://doi.org/10.1016/j.watbs.2022.100041>.
- Xu, X.W.H., Fu, G.H., Zou, X.Q., Ge, C.D., Zhao, Y.F., 2017. Diurnal variations of carbon dioxide, methane, and nitrous oxide fluxes from invasive *Spartina alterniflora* dominated coastal wetland in northern Jiangsu Province. *Acta Oceanol. Sin.* 36, 105–113. <https://doi.org/10.1007/s13131-017-1015-1>.
- Xu, Y.J., Xu, Z., Yang, R.J., 2019. Rapid daily change in surface water pCO<sub>2</sub> and CO<sub>2</sub> evasion: a case study in a subtropical eutrophic lake in Southern USA. *J. Hydrol.* 570, 486–494. <https://doi.org/10.1016/j.jhydrol.2019.01.016>.
- Yang, P., Lai, D.Y.F., Huang, J.F., Tong, C., 2018a. Effect of drainage on CO<sub>2</sub>, CH<sub>4</sub>, and N<sub>2</sub>O fluxes from aquaculture ponds during winter in a subtropical estuary of China. *J. Environ. Sci.* 65, 72–82. <https://doi.org/10.1016/j.jes.2017.03.024>.
- Yang, P., Zhang, Y.F., Lai, D.Y.F., Tan, L.S., Jin, B.S., Tong, C., 2018b. Fluxes of carbon dioxide and methane across the water-atmosphere interface of aquaculture shrimp ponds in two subtropical estuaries: the effect of temperature, substrate, salinity and nitrate. *Sci. Total Environ.* 635, 1025–1035. <https://doi.org/10.1016/j.scitotenv.2018.04.102>.
- Yang, P., Lai, D.F., Yang, H., Tong, C., 2019. Carbon dioxide dynamics from sediment, sediment-water interface and overlying water in the aquaculture shrimp ponds in subtropical estuaries, southeast China. *J. Environ. Manag.* 236, 224–235. <https://doi.org/10.1016/j.jenvman.2019.01.088>.
- Yang, P., Huang, J.F., Yang, H., Penuelas, J., Tang, K.W., Lai, D.Y.F., et al., 2021. Diffusive CH<sub>4</sub> fluxes from aquaculture ponds using floating chambers and thin boundary layer equations. *Atmos. Environ.* 253, 10. <https://doi.org/10.1016/j.atmosenv.2021.118384>.
- Yang, P., Tang, K.W., Yang, H., Tong, C., Yang, N., Lai, D.Y.F., et al., 2022. Insights into the farming-season carbon budget of coastal earthen aquaculture ponds in southeastern China. *Agric. Ecosyst. Environ.* 335, 11. <https://doi.org/10.1016/j.agee.2022.107995>.
- Ye, W.W., Sun, H., Li, Y.H., Zhang, J.X., Zhang, M.M., Gao, Z.Y., et al., 2022. Greenhouse gas emissions from fed mollusk mariculture: a case study of a *Sinonovacula constricta* farming system. *Agric. Ecosyst. Environ.* 336. <https://doi.org/10.1016/j.agee.2022.108029>.
- Yu, P.S., Yang, X.F., Wang, B., Li, T., Tao, B.Y., Zheng, M.H., et al., 2022. Moderate CO<sub>2</sub> sink due to phytoplankton bloom following a typhoon passage over the East China Sea. *Cont. Shelf Res.* 238. <https://doi.org/10.1016/j.csr.2022.104696>.
- Yuan, J.J., Xiang, J., Liu, D.Y., Kang, H., He, T.H., Kim, S., et al., 2019. Rapid growth in greenhouse gas emissions from the adoption of industrial-scale aquaculture. *Nat. Clim. Change* 9, 318–322. <https://doi.org/10.1038/s41558-019-0425-9>.
- Zhang, D.X., Xu, W.J., Wang, F., He, J., Chai, X.R., 2022a. Carbon dioxide fluxes from mariculture ponds with swimming crabs and shrimps in eastern China: The effect of adding razor clams. *Aquac. Rep.* 22. <https://doi.org/10.1016/j.aqrep.2021.100917>.
- Zhang, M., Xiao, Q., Zhang, Z., Gao, Y., Zhao, J., Pu, Y., et al., 2019. Methane flux dynamics in a submerged aquatic vegetation zone in a subtropical lake. *Sci. Total Environ.* 672, 400–409. <https://doi.org/10.1016/j.scitotenv.2019.03.466>.
- Zhang, Y.F., Tang, K.W., Yang, P., Yang, H., Tong, C., Song, C.C., et al., 2022b. Assessing carbon greenhouse gas emissions from aquaculture in China based on aquaculture system types, species, environmental conditions and management practices. *Agric. Ecosyst. Environ.* 338, 108110 <https://doi.org/10.1016/j.agee.2022.108110>.
- Zhang, Y.P., Qin, Z.C., Li, T.T., Zhu, X.D., 2022c. Carbon dioxide uptake overrides methane emission at the air-water interface of algae-shellfish mariculture ponds: evidence from eddy covariance observations. *Sci. Total Environ.* 815, 152867 <https://doi.org/10.1016/j.scitotenv.2021.152867>.
- Zhao, J.Y., Zhang, M., Xiao, W., Wang, W., Zhang, Z., Yu, Z., et al., 2019. An evaluation of the flux-gradient and the eddy covariance method to measure CH<sub>4</sub>, CO<sub>2</sub>, and H<sub>2</sub>O fluxes from small ponds. *Agric. For. Meteorol.* 275, 255–264. <https://doi.org/10.1016/j.agrformet.2019.05.032>.
- Zhao, J.Y., Zhang, M., Xiao, W., Jia, L., Zhang, X.F., Wang, J., et al., 2021. Large methane emission from freshwater aquaculture ponds revealed by long-term eddy covariance observation. *Agric. For. Meteorol.* 308, 12. <https://doi.org/10.1016/j.agrformet.2021.108600>.
- Zhu, X.D., Hou, Y.W., Weng, Q.H., Chen, L.Z., 2019. Integrating UAV optical imagery and LiDAR data for assessing the spatial relationship between mangrove and inundation across a subtropical estuarine wetland. *ISPRS J. Photogramm. Remote Sens.* 149, 146–156. <https://doi.org/10.1016/j.isprsjprs.2019.01.021>.
- Zhu, X.D., Hou, Y.W., Zhang, Y.G., Lu, X.L., Liu, Z.Q., Weng, Q.H., 2021a. Potential of sun-induced chlorophyll fluorescence for indicating mangrove canopy photosynthesis. *J. Geophys. Res. Biogeosciences* 126 <https://doi.org/10.1029/2020JG006159>.
- Zhu, X.D., Sun, C.Y., Qin, Z.C., 2021b. Drought-induced salinity enhancement weakens mangrove greenhouse gas cycling. *J. Geophys. Res.: Biogeosciences* 126. <https://doi.org/10.1029/2021JG006416>.
- Zhu, X.D., Qin, Z.C., Song, L.L., 2021c. How land-sea interaction of tidal and sea breeze activity affect mangrove net ecosystem exchange. *J. Geophys. Res. Atmospheres* 126. <https://doi.org/10.1029/2020jd034047>.